

## Fabrication of Fluorescent Silica Nanoparticles Hybridized with AIE Luminogens and Exploration of Their Applications as Nanobiosensors in Intracellular Imaging\*\*

Mahtab Faisal,<sup>[a, b]</sup> Yuning Hong,<sup>[a, b]</sup> Jianzhao Liu,<sup>[a, b]</sup> Yong Yu,<sup>[a, b]</sup> Jacky W. Y. Lam,<sup>[a, b]</sup> Anjun Qin,<sup>[a, c]</sup> Ping Lu,<sup>[a, b]</sup> and Ben Zhong Tang\*<sup>[a, b, c]</sup>

**Abstract:** Highly emissive inorganic-organic nanoparticles with core-shell structures are fabricated by a one-pot, surfactant-free hybridization process. The surfactant-free sol-gel reactions of tetraphenylethene- (TPE) and silole-functionalized siloxanes followed by reactions with tetraethoxysilane afford fluorescent silica nanoparticles FSNP-1 and FSNP-2, respectively. The FSNPs

are uniformly sized, surface-charged and colloidally stable. The diameters of the FSNPs are tunable in the range of 45–295 nm by changing the reaction

**Keywords:** aggregation-induced emission • cell imaging • fluorescence • nanoparticles • sol-gel reaction

conditions. Whereas their TPE and silole precursors are non-emissive, the FSNPs strongly emit in the visible vision, as a result of the novel aggregation-induced emission (AIE) characteristics of the TPE and silole aggregates in the hybrid nanoparticles. The FSNPs pose no toxicity to living cells and can be utilized to selectively image cytoplasm of HeLa cells.

### Introduction

Fluorescent nanoparticles have been found useful as visualization tools for biological sensing, probing, imaging, monitoring.<sup>[1,2]</sup> Among nanoparticles, semiconductor quantum dots (QDs) have attracted much attention, particularly in

the area of cellular marking or imaging. QDs enjoy such advantages as size-tunable emission color, long luminescence lifetime and resistance to photobleaching. Their surfaces, however, need to be modified in order to improve their hydrophilicity. Recent investigations have revealed that a large portion (>40%) of QDs used under biological conditions show dark state. The use of high concentrations of QDs may solve this problem but causes more serious problems such as enhanced cytotoxicity. This is easy to understand, taking into consideration that QDs are usually chalcogenides of heavy metals (e.g., ZnSe, CdS and PdTe), which are well known toxicants or carcinogens.<sup>[3–6]</sup>

In contrast, silica nanoparticles (SNPs) are hydrophilic and biocompatible. SNPs have found a variety of applications in areas spanning from information technology to biological engineering. Besides being cytophilic, SNPs are transparent but nonfluorescent and hence ideal host materials for the fabrication of fluorescent silica nanoparticles (FSNPs) for imaging purposes. FSNPs can be prepared by incorporating fluorophores into silica networks via physical processes or chemical reactions. The silica matrix acts as a protective shield, reducing the likelihood of penetrations of oxygen and other harmful species that may cause photobleaching of the embedded fluorophores.<sup>[7–9]</sup>

For sensitive detection, trace analysis, diagnostic assay, and real-time monitoring, FSNPs should emit intense visible

[a] M. Faisal, Y. Hong, J. Liu, Y. Yu, Dr. J. W. Y. Lam, Dr. A. Qin, Dr. P. Lu, Prof. Dr. B. Z. Tang  
Department of Chemistry, Bioengineering Graduate Program  
Nano Science and Technology Program  
Institute of Molecular Functional Materials  
The Hong Kong University of Science & Technology (HKUST)  
Clear Water Bay, Kowloon, Hong Kong (China)  
Fax: (+852)2358-1594  
E-mail: tangbenz@ust.hk

[b] M. Faisal, Y. Hong, J. Liu, Y. Yu, Dr. J. W. Y. Lam, Dr. P. Lu, Prof. Dr. B. Z. Tang  
HKUST Fok Ying Tung Research Institute  
Nansha, Guangzhou 511458 (China)

[c] Dr. A. Qin, Prof. Dr. B. Z. Tang  
Department of Polymer Science and Engineering  
Institute of Biomedical Macromolecules, Zhejiang University  
Hangzhou 310027 (China)

[\*\*] AIE = aggregation-induced emission.

Supporting information for this article is available on the WWW under <http://dx.doi.org/10.1002/chem.200901823>.

light upon photoexcitation. However, light emission from most of the FSNPs prepared thus far have been rather weak. This is due to the emission quenching caused by the aggregation of fluorophores in the solid state.<sup>[10]</sup> A low fluorophore loading in the nanoparticle may be free of aggregation but can offer only weak fluorescence signals. The light emission can further be weakened, rather than enhanced, when more fluorophores are loaded into the nanoparticles, because of the notorious aggregation-caused quenching (ACQ) effect.<sup>[11]</sup>

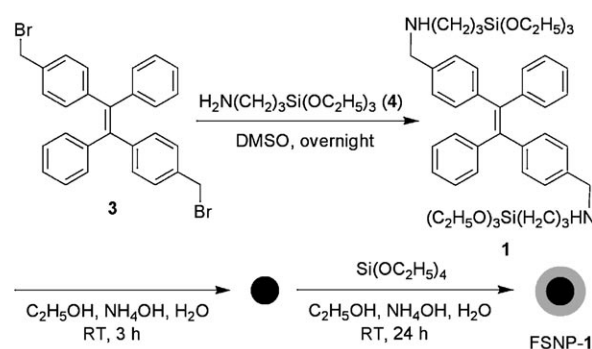
We have discovered an “abnormal” phenomenon that is exactly opposite to the ACQ effect, namely aggregation-induced emission (AIE). Nonemissive luminogens, such as tetraphenylethene (TPE) and hexaphenylsilole, are induced to emit efficiently by aggregate formation.<sup>[12–14]</sup> The AIE effect dramatically boosts fluorescence quantum yields ( $\Phi_F$ ) of the luminogens, turning them from faint fluorophores to strong emitters. An extreme example of such AIE luminogen is 4,4'-bis(1,2,2-triphenylvinyl)biphenyl: its emission efficiencies in the solution ( $\Phi_{FS}$ ) and aggregate ( $\Phi_{FA}$ ) states are ~0 and 100%, respectively, resulting in an infinitely large AIE effect ( $\alpha_{AIE} = \Phi_{FA}/\Phi_{FS} \rightarrow \infty$ ).<sup>[12]</sup> Mechanistic investigations reveal that the AIE effect is caused by the restriction to the intramolecular rotations of the luminogens in the aggregate state.<sup>[15–19]</sup> The AIE effect has enabled the luminogens to find an array of technological applications as chemosensors, bioprobes, PAGE visualizers, active layers in the construction of organic light-emitting diodes.<sup>[15]</sup>

In this work, we explored the possibility of hybridizing the AIE luminogens with silica gels with the aim of fabricating emissive FSNPs. Although microemulsion process has been widely used for the preparations of FSNPs, it involves tedious syntheses of dye-doped silica cores followed by deposition of pure silica shells.<sup>[20]</sup> Surfactants are needed in the process to generate nanodimensional templates. The resultant FSNPs thus must be thoroughly washed prior to biological applications, because surfactants are harmful to living cells.<sup>[21]</sup> Unfortunately, however, the surfactant coatings on the FSNPs are extremely difficult, if not impossible, to clean up.

In this paper, we report our work on the syntheses of AIE-active FSNPs with core-shell structures through a surfactant-free sol-gel process in a one-pot experimental procedure. In our approach, the luminogens are chemically bound to, rather than physically blended with, the silica networks. The AIE luminogens thus do not leak out from the FSNPs.<sup>[22–24]</sup> We obtained FSNPs with uniform sizes, high surface charges and excellent colloidal stability. Thanks to the AIE nature of the luminogen nanoaggregates and the biocompatibility of the silica gels, the FSNPs emit strong visible lights and pose no cytotoxicity, which make them promising fluorescent biomarkers for cell imaging.

## Results and Discussion

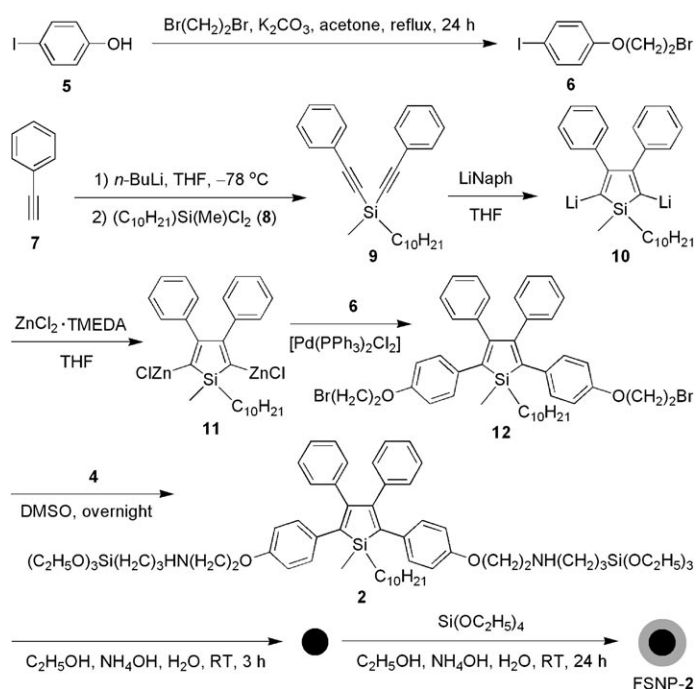
**Fabrication of FSNPs:** With a view to fabricating FSNPs with strong light emissions in the solid state, we prepared di-brominated TPE and silole derivatives **3** and **12** with AIE attribute (Schemes 1 and 2). While **3** was prepared following our previously published experimental procedures,<sup>[13,18]</sup> the synthetic route to **12** is given in Scheme 2. Compound **6** is first prepared by the etherization of 4-iodophenol (**5**) with 1,2-dibromoethane. The lithiation of phenyl-acetylene (**7**) followed by reaction with dichlorosilane **8** produces bis(phenylethynyl)silane (**9**), which reacts with an excess amount of lithium 1-naphthalenide to form 2,5-dilithio-silole **10**. Transmetalation of **10** with  $ZnCl_2 \cdot TMEDA$  affords 2,5-dizincated silole **11**, treatment of which with **6** in the presence of a palladium catalyst yields **12**.



Scheme 1. Fabrication of TPE-containing fluorescent silica nanoparticles FSNP-1. Abbreviation: TPE = tetraphenylethene, DMSO = dimethyl sulfoxide.

To covalently bind the AIE luminogens to SNPs at molecular level, we employed (3-aminopropyl)triethoxysilane (APS or **4**) as a chemical linker. As shown in Scheme 1, the APS–TPE adduct **1** is prepared by stirring a mixture of APS and **3** in distilled DMSO at room temperature overnight under stringently dry conditions. The reaction product gives an  $[M^+ + 1]$  peak at  $m/z$  799.4536 in its high-resolution mass spectrum (HRMS), as shown in Figure S1 in the Supporting Information, confirming the occurrence of the coupling reaction and the formation of expected adduct **1** ( $m/z$  798.4459  $[M^+]$ ). The sol-gel reaction of **1** catalyzed by ammonium hydroxide is carried out in an aqueous mixture at room temperature for 3 h. The resultant TPE-silica nanocore is then subjected to further sol-gel reaction with tetraethyl orthosilicate (TEOS), yielding FSNP-1 with the luminogen core coated with a silica shell. Similarly, coupling of APS with **12** affords adduct **2** and its two-step sol-gel reaction in a one-pot procedure results in the formation of FSNP-2 with a core-shell structure (Scheme 2).

The atomic compositions of the obtained FSNPs were estimated by energy dispersive X-ray spectroscopy (EDX) and the results are given in Table S1 in the Supporting Information. Analysis by  $\xi$  potential analyzer at room temperature



Scheme 2. Synthesis of silole derivative **2** and fabrication of its fluorescent silica nanoparticles FSNP-2. Abbreviation: Naph = 1-naphthyl, THF = tetrahydrofuran, TMEDA = *N,N,N',N'*-tetramethylethylenediamine.

shows that the FSNPs are monodispersed with polydispersity down to 0.005 (Figure 1). The average diameters of FSNP-1 and FSNP-2 are 206.3 and 225.0 nm, respectively, which are somewhat larger than those measured by transmission electron microscopy (TEM): 175 and 200 nm for FSNP-1 and FSNP-2, respectively, due to swelling of the FSNPs in aqueous mixtures and their shrinkage under the high vacuum in the TEM chamber.<sup>[25,26]</sup>

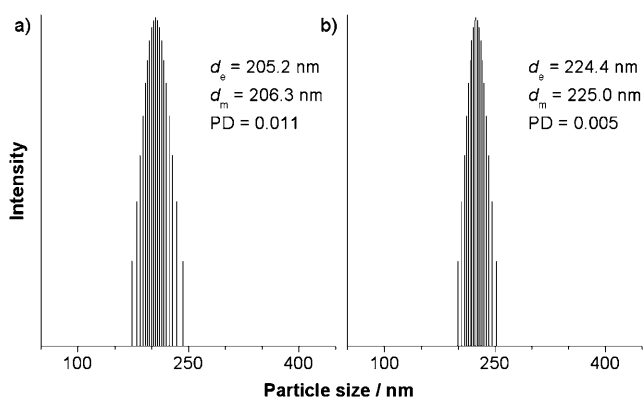


Figure 1. Particle size distributions of a) FSNP-1 and b) FSNP-2. Abbreviation:  $d_e$  = effective diameter,  $d_m$  = mean diameter, PD = polydispersity.

**Light emission:** Figure 2 shows fluorescence spectra of solutions of **1** and **2** and suspensions of their core-shell nanoparticles FSNP-1 and FSNP-2 in ethanol. The spectra of the

pure SNPs containing no luminogens prepared under the similar conditions are shown in the figures for comparison. Nearly no fluorescence signals are recorded when the SNPs are photoexcited. Similarly the fluorescence spectra of **1** and **2** are almost flat lines parallel to the abscissas. In the dilute ethanol solutions, the multiple peripheral aryl rings in the isolated molecules of luminogens **1** and **2** undergo active intramolecular rotations, which effectively annihilate their excited states and hence render them nonemissive.<sup>[27–30]</sup>

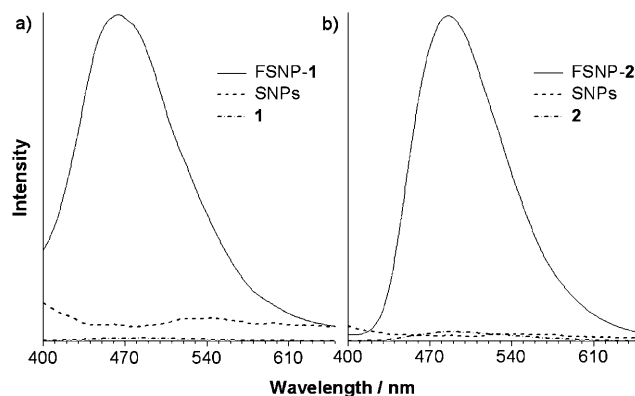


Figure 2. Fluorescence spectra of a) FSNP-1 and **1** and b) FSNP-2 and **2** in ethanol. The spectra of SNPs are shown for comparison. Concentration of luminogen: a) 4  $\mu\text{M}$ , b) 3  $\mu\text{M}$ ; excitation wavelength: a) 353 nm, b) 371 nm.

When the molecules of **1** and **2** are covalently incorporated into, and aggregate in, the silica networks, strong fluorescence spectra peaked at 465 and 485 nm, respectively, are recorded, confirming that **1** and **2**, similar to their respective congeners **3** and **12**, are AIE active.<sup>[13,18]</sup> The rigid silica networks largely restrict intramolecular rotations in the luminogens. This blocks the nonradiative relaxation channel and populates the radiative decay, thus making the FSNPs highly luminescent.

By dissolving **1** and **2** and dispersing FSNP-1 and FSNP-2 with the same molar quantities of luminogens in ethanol, their emission intensities are compared. The light emissions from FSNP-1 and FSNP-2 are 135- and 60-fold more intense than those from **1** and **2**, respectively. The  $\Phi_F$  values of FSNPs with different loadings of luminogens manifest the salient feature of AIE (Table 1): they do not suffer from the ACQ effect and their fluorescence efficiencies are increased with an increase in the luminogen loading. The light emis-

Table 1. Fluorescence quantum yields ( $\Phi_F$ ) of fluorescent silica nanoparticles<sup>[a]</sup>

Content of luminogen [ $\mu\text{mol}$ ]	FSNP-1	$\Phi_F$ [%]	FSNP-2
4	17.6		13.5
8	21.9		23.3
12	30.1		39.0

[a] Absolute values determined by integrating sphere.

sion is very stable, with no change in the fluorescence spectra detectable after the FSNPs have been put on shelves for several months without protecting from light and air.

Figure 3 shows images of the solutions of **1** and **2** and the suspensions of FSNP-1 and FSNP-2 as well as SNPs taken upon exposure to the irradiation with a UV lamp. Whereas the solutions of **1** and **2** and the suspensions of SNPs are invisible under the UV illumination, intense blue and green light is emitted from FSNP-1 and FSNP-2, respectively. This visual observation further supports that the intramolecular rotations of **1** and **2** are restricted by the covalent melding of the AIE luminogens with the silica matrix.

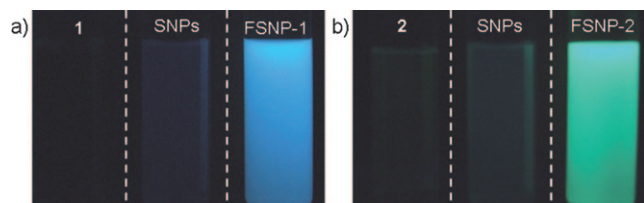


Figure 3. Solutions and suspensions of a) **1**, SNPs and FSNP-1 and b) **2**, SNPs and FSNP-2 in ethanol; photographs taken upon irradiation with a UV light of 365 nm. Whereas **1**, **2** and SNPs are invisible under the UV illumination, strong blue and green lights are emitted from FSNP-1 and FSNP-2, respectively.

**Colloidal stability:** The  $\xi$  potential analyses reveal that the FSNPs, similar to SNPs, possess high surface charges and hence excellent colloidal stability.<sup>[31]</sup> The  $\xi$  potential of pure SNPs is negatively signed, whose absolute value is increased with an increase in pH of the aqueous medium (Supporting Information, Figure S3). At high pH value or in the basic medium, the acidic hydroxyl groups on the nanoparticle surfaces are converted into basic form, imparting high surface charges and hence good stability to the SNPs.

The FSNPs, however, exhibit positively signed  $\xi$  potentials at pH 2 due to the protonation of the amino groups contributed from the APS moieties.<sup>[32,33]</sup> At higher pH values, this event is less likely to occur but the dissociation of hydroxyl groups is favored. This explains why the  $\xi$  potentials of the FSNPs change to negative sign and are increased in the aqueous media with high or low pH values. Although the  $\xi$  potential of FSNP-1 is different from that of FSNP-2 because some of the free APS moieties are present on the particle surfaces but the general trend is the same for both of the FSNPs.

**Size tunability:** It is important to tailor the sizes of nanoparticles to meet the requirements of different technological applications. By varying the reaction conditions, we can manipulate the sizes of the FSNPs. The FSNPs with smaller diameters are obtained when the sol-gel reactions are carried out in the presence of smaller amounts of ammonium hydroxide, while higher concentrations of TEOS and ammonium hydroxide promote the formation of FSNPs with larger particle sizes.

TEM and scanning electron microscope (SEM) images show that all the nanoparticles prepared are uniform in diameters with narrow size distributions and smooth surfaces (Figures 4 and 5). These results are consistent with those obtained from the  $\xi$  potential analyses of their suspensions in the aqueous media (Table 2), in which the FSNPs practically do not agglomerate and thus show their intrinsically low polydispersities (down to 0.005).

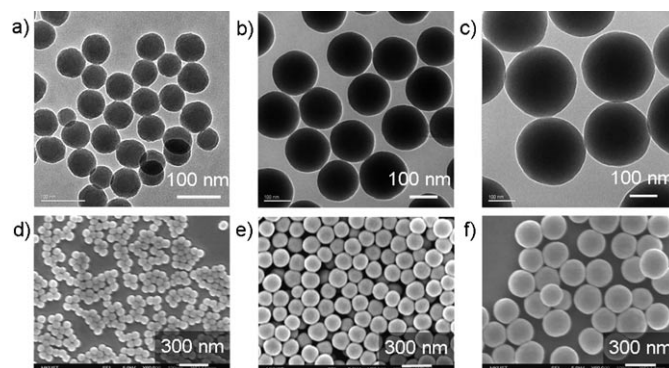


Figure 4. a)–c) TEM and d)–f) SEM images of monodispersed FSNP-1 with different particle sizes: a) and d) 60 nm, b) and e) 175 nm, and c) and f) 250 nm.

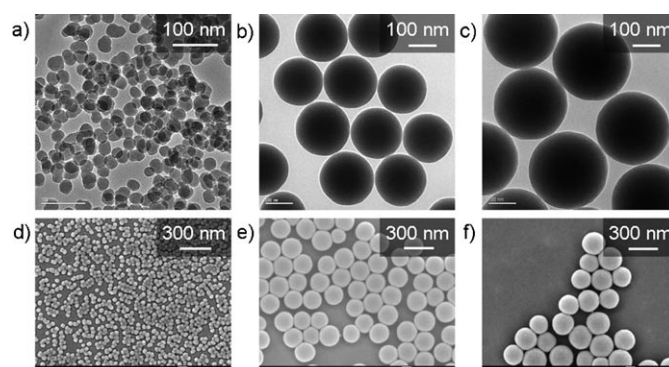


Figure 5. a)–c) TEM and d)–f) SEM images of monodispersed FSNP-2 with different particle sizes: a) and d) 45 nm, b) and e) 200 nm, and c) and f) 270 nm.

Table 2. Particle sizes and polydispersities of fluorescent silica nanoparticles.<sup>[a]</sup>

FSNP-1		FSNP-2	
<i>d</i> [nm]	PD	<i>d</i> [nm]	PD
86.3	0.027	58.1	0.167
206.3	0.011	225.0	0.005
295.0	0.005	280.6	0.005

[a] Determined by  $\xi$  potential analysis; *d* = diameter, PD = polydispersity.

**Cell imaging:** To serve as a useful biological tracer, a luminogen should neither inhibit nor promote the growth of living cells.<sup>[15]</sup> As can be seen from Figures S4 and S5 (Supporting Information), in the presence of the TPE and silole derivatives **3** and **12**, the HeLa cells grow similar as in the

control experiments in the absence of the luminogens. Evidently, **3** and **12** exert no toxicity on the living cells. In other words, they are cytocompatible without interfering with the metabolisms of the cells.

The TPE and silole derivatives **3** and **12** are the precursors to the AIE luminogens **1** and **2**, respectively, and their biocompatibilities prompt us to explore the possibility of utilizing FSNP-1 and FSNP-2 for cell-imaging applications. As shown in Figure 6, the AIE-active FSNPs selectively stain the cytoplasmic regions of the living cells. The brightness of the fluorescence images of the cells is increased with an increase in the luminogen loading in the FSNPs.

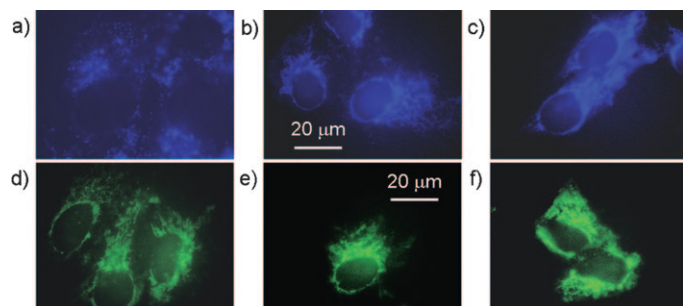


Figure 6. Fluorescence images of HeLa cells stained by a)–c) FSNP-1 and d)–f) FSNP-2 with different luminogen loadings. Concentration of luminogen [ $\mu\text{M}$ ]: a) 2, b) 4, c) 8, d) 2, e) 4, f) 6.

The major route for the FSNPs to enter the living cells is through endocytosis, with the amino groups on the particle surfaces further facilitating the cellular uptake.<sup>[20]</sup> The FSNPs are enclosed by the cell membranes to form small vesicles, which are then internalized by the cells. The FSNPs are further processed in endosomes and lysosomes and are eventually released to the cytoplasm.<sup>[34–36]</sup> When bound to the biomacromolecules, the FSNPs may emit even more intensely, because the intramolecular rotations in the luminogenic moieties are further restricted if some of them are located on the nanoparticle surfaces.<sup>[37]</sup> Although the silica shells are hydrophilic, no fluorescence is observed in the cell nucleus, probably due to the “large” sizes of the FSNPs.

The AIE luminogens can be excited by a two-photon process, which enables the use of excitation wavelengths with lower energies and higher benignancy to living cells. Further studies on the two-photon fluorescence processes of the FSNPs and their bioimaging applications are in progress in collaborations with our physicist and bioengineering colleagues.

## Conclusion

In this work, we have developed a simple process for the syntheses of highly emissive FSNPs with core-shell structures. The process does not use surfactant stabilizers and involves a two-step sol-gel reaction in a one-pt experimental procedure. The resultant FSNPs are monodispersed with

smooth surfaces. They possess high surface charges and hence excellent colloidal stability. Whilst the solutions of **1** and **2** in ethanol are nonemissive, the suspensions of FSNP-1 and FSNP-2 in the aqueous medium emit strong blue and green lights, respectively, upon photoexcitation, thanks to their novel AIE attributes. The particle diameters and emission efficiencies of the FSNPs are manipulable by changing the reaction conditions and luminogen loadings. The FSNPs pose no toxicity to living cells and function as fluorescent visualizers for intracellular imaging.

We are now investigating multi-photon luminescence processes of the FSNPs and their surface modifications via bioconjugations with (macro)molecules of biological origin to enhance their binding specificities and sensing selectivities. We are also working on the introduction of magnetic components to the inner cores of the core-shell particles, in an effort to prepare nanostructured materials that show high fluorescence efficiency and magnetic susceptibility. The results on the fabrication of fluorescent and magnetic particles and their biotechnological applications have been briefly discussed in one of our recent reviews;<sup>[38]</sup> full experimental details will be reported in a separate paper in due course.

## Experimental Section

**Materials:** THF was purchased from Labscan and purified by simple distillation from sodium/benzophenone under nitrogen immediately prior to use. TEOS, DMSO, APS, phenylacetylene, *n*-butyllithium, naphthalene, decylmethylchlorosilane, lithium, dichloro(*N,N,N'*-tetramethylethylenediamine)zinc, 4-iodophenol, 1,2-dibromoethane, dichlorobis(triphenylphosphine)palladium(II) and other reagents were all purchased from Aldrich and used as received. 1,2-Bis(4-bromomethylphenyl)diphenylethene (**3**) was prepared using our previously reported procedures.<sup>[13,18]</sup>

**Instrumentations:** <sup>1</sup>H and <sup>13</sup>C NMR spectra were recorded on a Bruker ARX 400 spectrometer with tetramethylsilane (TMS;  $\delta=0$ ) as internal standard. HRMS spectra were recorded on a Finnigan TSQ 7000 triple quadrupole spectrometer operating in a MALDI-TOF mode. The morphologies of the FSNPs were investigated using JOEL 2010 TEM and JOEL 6700F SEM at an accelerating voltage of 200 and 5 kV, respectively. Samples were prepared by drop-casting dilute dispersions of the FSNPs onto copper 400-mesh carrier grids covered with carbon-coated formvar films. The solvent was evaporated at room temperature in open air. Fluorescence spectra were taken on a Perkin-Elmer LS 50B spectrofluorometer with a Xenon discharge lamp excitation.  $\xi$  potentials and particle sizes of the FSNPs were determined at room temperature by a ZetaPlus Potential Analyzer (Brookhaven Instruments Corporation, USA).

**1-(2-Bromoethoxy)-4-iodobenzene (6):** To a mixture of 4-iodophenol (5.0 g, 22.7 mmol) and potassium carbonate (4.7 g, 34.1 mmol) in acetone was added 12.8 g (68.2 mmol) of 1,2-dibromoethane. The mixture was stirred and heated to reflux for 24 h. After filtration and solvent evaporation, the crude product was purified by silica gel chromatography using chloroform/hexane 1:4. The product was obtained as white powder (5.8 g, 78%). <sup>1</sup>H NMR (400 MHz, CDCl<sub>3</sub>, TMS):  $\delta$  = 7.57 (d, 2H), 6.69 (d, 2H), 4.25 (t, 2H), 3.62 ppm (t, 2H); <sup>13</sup>C NMR (100 MHz, CDCl<sub>3</sub>, TMS):  $\delta$  = 158.0, 138.3, 117.1, 83.6, 67.9, 28.8 ppm.

**Bis(phenylethynyl)decylmethylsilane (9):** *n*BuLi (25.0 mL, 40.1 mmol, 1.6M solution in hexane) was added at  $-78^\circ\text{C}$  to a THF solution of **7** (4.0 mL, 36.4 mmol). After stirring at the same temperature for 2 h, decylmethylchlorosilane (4.8 mL, 18.2 mmol) was added at  $-78^\circ\text{C}$ . The mixture was warmed to room temperature and stirred overnight. The solvent was removed under reduced pressure. The mixture was dissolved in

dichloromethane and washed with water. The organic layer was dried over magnesium sulfate and filtered. The filtrate was evaporated and the crude product was purified by a silica gel column using hexane. Product **9** was obtained as colorless liquid (12.42 g, 82%).  $^1\text{H NMR}$  (400 MHz,  $\text{CDCl}_3$ , TMS):  $\delta$  = 7.60 (m, 4H), 7.40 (m, 6H), 1.73–1.69 (t, 2H), 1.56 (m, 2H), 1.38 (m, 12H), 1.03–0.98 (m, 5H), 0.57 ppm (s, 3H);  $^{13}\text{C NMR}$  (100 MHz,  $\text{CDCl}_3$ , TMS):  $\delta$  = 132.1, 128.7, 128.1, 122.8, 106.3, 90.0, 32.9, 31.9, 29.6, 29.5, 29.3, 29.2, 23.6, 22.7, 16.2, 14.1, 1.2 ppm.

#### 1-Decyl-1-methyl-2,5-bis[4-(2-bromoethoxy)phenyl]-3,4-diphenylsilole

**(12)**: A mixture of lithium (0.056 g, 8 mmol) and naphthalene (1.04 g, 8 mmol) in THF (8 mL) was stirred at room temperature under nitrogen for 3 h to form a deep dark green solution of lithium 1-naphthalenide. The viscous solution was added dropwise to a solution of **9** (0.77 g, 2 mmol) in THF (5 mL) over 2 min at room temperature. After stirring for 1 h, the mixture was cooled to 0°C with an ice bath and diluted with THF (10 mL).  $\text{ZnCl}_2\cdot\text{TMEDA}$  (2 g, 8 mmol) was then added to the mixture to give a black suspension. After stirring for an additional hour at room temperature, a solution of **6** (1.63 g, 4.9 mmol) and  $[\text{PdCl}_2(\text{PPh}_3)_2]$  (0.08 g, 0.1 mmol) in THF (10 mL) was added. The mixture was refluxed overnight. After cooling to room temperature, 3M HCl solution (10 mL) was added and the mixture was extracted with dichloromethane. The combined organic layer was washed with brine and dried over magnesium sulfate. After solvent evaporation under reduced pressure, the residue was purified by a silica gel column using ethyl acetate/hexanes 1:9. The product was obtained as a yellow liquid (0.78 g, 50%).  $^1\text{H NMR}$  (400 MHz,  $\text{CDCl}_3$ , TMS):  $\delta$  = 7.03 (t, 6H), 6.87–6.81 (m, 8H), 6.70–6.66 (m, 4H), 4.24–4.15 (m, 4H), 3.77 (t, 1H), 3.60 (t, 1H), 3.38 (t, 2H), 1.46–1.21 (m, 16H), 1.03–0.99 (t, 2H), 0.91–0.88 (t, 4H), 0.47 ppm (s, 3H);  $^{13}\text{C NMR}$  (100 MHz,  $\text{CDCl}_3$ , TMS):  $\delta$  = 156.0, 155.9, 155.8, 153.9, 139.5, 139.3, 133.2, 133.1, 130.2, 129.9, 127.5, 126.1, 114.3, 114.2, 114.1, 68.5, 67.7, 41.9, 32.9, 31.9, 29.6, 29.5, 29.3, 29.1, 23.6, 22.7, 14.1, 14.0, 1.2, –5.0 ppm; HRMS (TOF):  $m/z$ : calcd for 788.1906; 788.3618  $[\text{M}]^+$ .

**Fabrications of FSNPs containing AIE luminogens**: TPE–APS adduct was prepared by stirring a mixture of 4  $\mu\text{M}$  of **3** and 10  $\mu\text{M}$  of APS in DMSO (100  $\mu\text{L}$ ) overnight. Water was carefully excluded to avoid possible hydrolysis of the APS moieties. The reaction mixture was concentrated under vacuum and the product (**1**) was characterized by mass spectroscopy (Supporting Information, Figure S1). The resultant TPE–APS adduct **1** was then used to prepare the TPE-containing FSNPs by a two-step sol–gel reaction. Thus, **1** was added into a mixture of ethanol (64 mL), ammonium hydroxide (1.28 mL) and distilled water (7.8 mL) and stirred at room temperature for 3 h to prepare the TPE–silica nanocores. A mixture of TEOS (2 mL) in ethanol (8 mL) was then added dropwise into the mixture of the nanocores and the reaction was stirred at room temperature for an additional 24 h to coat the luminogenic nanocores with silica shells.<sup>[59]</sup> After incubation, the mixture was centrifuged and the FSNP-**1** nanoparticles were redispersed in ethanol under sonication for 5 min. Such process was repeated three times and the final dispersion of FSNP-**1** in water was used for the cell imaging experiments. Similarly, the silole-APS adduct **2** was prepared by dehydrobromination coupling of **12** with APS and the FSNP-**2** nanoparticles were fabricated by sol–gel reaction of **2** catalyzed by ammonium hydroxide followed by coating of the resultant luminogenic nanocores by silica shells.

**Cell culture**: HeLa cells were cultured in minimum essential medium containing 10% fetal bovine serum and antibiotics (100 units per mL penicillin and 100  $\mu\text{g mL}^{-1}$  streptomycin) in a 5% carbon dioxide humidity incubator at 37°C. The cell proliferation Kit I (MTT) was used to measure the cell viability. First, 5000 cells were seeded per well in a 96-well plate. After overnight culture, various concentrations of **3** or **12** were added into the 96-well plate. After 24 h, 10  $\mu\text{L}$  of MTT solution (5  $\text{mg mL}^{-1}$  in PBS) was added into each well. After 2 h incubation at 37°C, 100  $\mu\text{L}$  of solubilization mixture containing 10% SDS and 0.01 M HCl was added to dissolve the purple crystals. After 24 h, the optical density readings at 595 nm were taken using a plate reader. Every experiment was performed at least three times.

**Cell imaging**: HeLa cells were grown overnight on a plasma-treated 25 mm round cover slip mounted onto a 35 mm Petri dish with an observation window. The living cells were stained with 250  $\mu\text{L}$  of FSNPs with

different concentrations and incubated for 24 h. The cells were imaged under an inverted fluorescence microscope (Nikon Eclipse TE2000-U;  $\lambda_{\text{ex}}$  = 330–380 nm, dichroic mirror = 400 nm). The images of the cells were captured using a digital CCD camera.

## Acknowledgements

This work was partially supported by the Hong Kong Research Grants Council (603008, HKUST13/CRF/08 and 602706), the National Science Foundation of China (20974028 and 20634020), the University Grants committee of Hong Kong (AoE/P-03/08) and the Ministry of Science & Technology (2009CB623605). B.Z.T. thanks the support from Cao Guangbiao Foundation of Zhejiang University.

- [1] K. P. Velikov, A. V. Blaaderen, *Langmuir* **2001**, *17*, 4779–4786.
- [2] C. Graf, A. V. Blaaderen, *Langmuir* **2002**, *18*, 524–534.
- [3] A. M. Derfus, W. C. W. Chan, S. N. Bhatia, *Nano Lett.* **2004**, *4*, 11–18.
- [4] J. Yao, D. Larson, H. Vishwasrao, W. Zipfel, W. Webb, *Proc. Natl. Acad. Sci. USA* **2005**, *102*, 14284–14289.
- [5] T. Pellegrino, S. Kudera, T. Liedl, A. Javier, L. Manna, W. Parak, *Small* **2005**, *1*, 48–63.
- [6] H. Ow, D. Larson, M. Srivastava, B. Baird, W. Webb, U. Wiesner, *Nano Lett.* **2005**, *5*, 113–117.
- [7] A. Burns, H. Ow, U. Wiesner, *Chem. Soc. Rev.* **2006**, *35*, 1028–1042.
- [8] L. Wang, W. Zhao, W. Tan, *Nano Res.* **2008**, *1*, 99–115.
- [9] S. Santra, K. Wang, R. Tapeç, W. Tan, *J. Biomed. Opt.* **2001**, *6*, 160–166.
- [10] M. Nakamura, M. Shono, K. Ishimura, *Anal. Chem.* **2007**, *79*, 6507–6514.
- [11] J. B. Birks, *Photophysics of Aromatic Molecules*, Wiley, New York, **1970**.
- [12] Z. Zhao, S. Chen, X. Shen, F. Mahtab, Y. Yu, P. Lu, J. W. Y. Lam, H. S. Kwok, B. Z. Tang, *Chem. Commun.* **2010**, 686–688.
- [13] Y. Hong, Y. Dong, H. Tong, M. Häußler, J. W. Y. Lam, B. Z. Tang, *Polym. Prepr. (Am. Chem. Soc. Div. Polym. Chem.)* **2007**, *48*, 367–368.
- [14] H. Tong, Y. Dong, Y. Hong, M. Haeussler, J. W. Y. Lam, H. H.-Y. Sung, X. Yu, J. Sun, I. D. Williams, H. S. Kwok, B. Z. Tang, *J. Phys. Chem. C* **2007**, *111*, 2287–2294.
- [15] Y. Hong, J. W. Y. Lam, B. Z. Tang, *Chem. Commun.* **2009**, 4332–4353.
- [16] J. Chen, B. Xu, X. Ouyang, B. Z. Tang, Y. Cao, *J. Phys. Chem. A* **2004**, *108*, 7522–7526.
- [17] H. Tong, Y. Hong, Y. Q. Dong, Y. Ren, M. Häußler, J. W. Y. Lam, K. S. Wong, B. Z. Tang, *J. Phys. Chem. B* **2007**, *111*, 2000–2007.
- [18] H. Tong, Y. Q. Dong, Y. Hong, M. Häußler, J. W. Y. Lam, H. H. Sung, X. Yu, J. Sun, I. D. Williams, H. S. Kwok, B. Z. Tang, *J. Phys. Chem. C* **2007**, *111*, 2287–2294.
- [19] H. Tong, Y. Hong, Y. Dong, M. Häußler, J. W. Y. Lam, Z. Li, Z. F. Guo, Z. H. Guo, B. Z. Tang, *Chem. Commun.* **2006**, 3705–3707.
- [20] R. Kumar, I. Roy, T. Y. Ohulchanskyy, L. N. Goswami, A. C. Bonoiu, E. J. Bergey, K. M. Tramosch, A. Maitra, Paras N. Prasad, *ACS Nano* **2008**, *2*, 449–456.
- [21] X. L. Chen, J. L. Zou, T. T. Zhao, Z. B. Li, *J. Fluoresc.* **2007**, *17*, 235–241.
- [22] A. van Blaaderen, J. V. Geest, A. Vrij, *J. Colloid Interface Sci.* **1992**, *154*, 481–501.
- [23] J. H. Zhang, P. Zhan, Z. L. Wang, W. Y. Zhang, N. B. Ming, *J. Mater. Res.* **2003**, *18*, 649–653.
- [24] K. S. Rao, K. El-Hami, T. Kodaki, K. Matsushige, K. Makino, *J. Colloid Interface Sci.* **2005**, *289*, 125–131.
- [25] N. A. M. Verhaegh, A. V. Blaaderen, *Langmuir* **1994**, *10*, 1427–1438.

- [26] V. Helden, A. K. Jansen, J. W. Vrij, *J. Colloid Interface Sci.* **1981**, *81*, 354–368.
- [27] H. Tong, Y. Dong, M. Häußler, Y. Hong, J. W. Y. Lam, H. H-Y. Sung, I. D. Williams, H. S. Kwok, B. Z. Tang, *Chem. Phys. Lett.* **2006**, *428*, 326–330.
- [28] J. Luo, Z. Xie, J. W. Y. Lam, L. Cheng, H. Chen, C. Qiu, H. S. Kwok, X. Zhan, Y. Liu, D. Zhu, B. Z. Tang, *Chem. Commun.* **2001**, 1740–1741.
- [29] H. J. Tracy, J. L. Mullin, W. T. Klooster, J. A. Martin, J. Haug, S. Wallace, I. Rudloe, K. Watts, *Inorg. Chem.* **2005**, *44*, 2003–2011.
- [30] Z. Ning, Z. Chen, Q. Zhang, Y. Yan, S. Qian, Y. Cao, H. Tian, *Adv. Funct. Mater.* **2007**, *17*, 3799–3807.
- [31] S. Kim, H. E. Pudavar, A. Bonoiu, P. N. Prasad, *Adv. Mater.* **2007**, *19*, 3791–3795.
- [32] R. M. Ottenbrite, J. S. Wall, *J. Am. Ceram. Soc.* **2000**, *83*, 3214–3215.
- [33] A. van Blaaderen, A. Vrij, *J. Colloid Interface Sci.* **1993**, *156*, 1–18.
- [34] S. D. Conner, S. L. Schmid, *Nature* **2003**, *422*, 37–44.
- [35] M. Marsh, H. T. McMahon, *Science* **1999**, *285*, 215–220.
- [36] M. Breunig, S. Bauer, A. Goepferich, *Eur. J. Pharm. Biopharm.* **2008**, *68*, 112–128.
- [37] W. Stöber, A. Fink, J. Bohn, *J. Colloid Interface Sci.* **1968**, *26*, 62–66.
- [38] J. Liu, J. W. Y. Lam, B. Z. Tang, *J. Inorg. Organomet. Polym. Mater.* **2009**, *19*, 249–285.
- [39] J. E. Fuller, G. T. Zugates, L. S. Ferreira, H. S. Ow, N. N. Nguyen, U. B. Wiesner, R. S. Langer, *Biomaterials* **2008**, *29*, 1526–1532.

Received: July 2, 2009  
Published online: March 2, 2010